Conical light scattering in strontium barium niobate crystals related to an intrinsic composition inhomogeneity

2007 J. Phys.: Condens. Matter 19 156225

(http://iopscience.iop.org/0953-8984/19/15/156225)

IOP PUBLISHING JOURNAL OF PHYSICS: CONDENSED MATTER

J. Phys.: Condens. Matter **19** (2007) 156225 (9pp) doi:10.1088/0953-8984/19/15/156225

Conical light scattering in strontium barium niobate crystals related to an intrinsic composition inhomogeneity

K Bastwöste, U Sander and M Imlau

Fachbereich Physik, Universität Osnabrück, Barbarastraße 7, D-49069 Osnabrück, Germany

E-mail: mimlau@uos.de

Received 21 December 2006, in final form 19 February 2007
Published 27 March 2007
Online at stacks.iop.org/JPhysCM/19/156225

Abstract

Conical light scattering is uncovered in poly- and mono-domain, nominally pure and Eu-doped strontium barium niobate (SBN) crystals over a wide temperature regime. The appearance of two scattering cones, a scattering line and a corona is observed and can be explained comprehensively within the Ewald sphere concept. Photorefraction, scattering from domain boundaries or from growth striations can be excluded from explaining the origin of the scattering. It is shown that the temperature-persistent scattering process is related to a growth-induced seeding rod, i.e. a composition inhomogeneity primarily localized at the centre of the SBN sample. The rod is directed parallel to the *c* axis and yields a refractive-index inhomogeneity with spatial frequencies on the micro-scale.

(Some figures in this article are in colour only in the electronic version)

1. Introduction

Conical light scattering, i.e. scattering of an incident coherent light beam onto the surface of a cone, has been reported for natural crystals of tourmaline [1], polar oxides including doped $LiNbO_3$ [2, 3] or $Sr_{0.61}Ba_{0.39}Nb_2O_6$ (SBN) [4], and for molecular crystals of $Na_2[Fe(CN)_5NO]\cdot 2H_2O$ [5] as well. A strict dependence of the cone apex angle on the angle of the incident probe light with respect to the crystal system is distinctive. The scattering is ascribed to the interaction of the incident light wave with a refractive-index inhomogeneity on the micro-scale in the crystal bulk. The origin of the related refractive-index inhomogeneity, however, is due to either impurity ions (scattering ring in tourmaline [1]), the presence of intrinsic (non-collinear frequency doubling [3, 6] or photoinduced ferroelectric domains [7]) or to volume phase gratings recorded via the photorefractive effect ('Venetian blind' effect [8], or polarization-anisotropic photoinduced light scattering [4]). The relation of conical light scattering to ferroelectric domains has enabled phase transition studies of

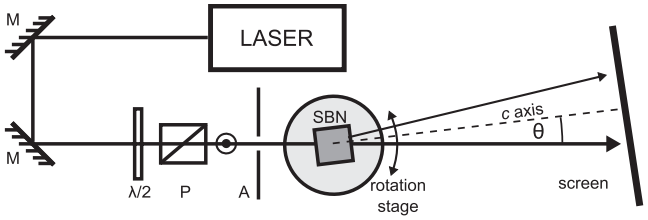

Figure 1. Experimental setup for the investigation of conical light scattering. The probe beam (Ar–Kr-ion laser) had a power of 50 mW and ordinary light polarization. M: Mirrors, $\lambda/2$: half-wave plate, P: polarizer, A: aperture.

the relaxor-ferroelectric SBN:Ce by determining the scattering intensity as a function of temperature [4]. Further, the apex angle of the scattering cone was applied to determine the Li/Nb ratio of Fe-doped $LiNbO_3$ crystals [2] and the composition inhomogeneity of Mg-doped $LiNbO_3$ samples [3].

In this paper we report on conical scattering observed in nominally pure and Eu-doped SBN which is related to a micro-scale refractive-index inhomogeneity that is intrinsic in the crystal bulk. Two scattering cones with marginal different apex angles $\alpha_{1,2}$ are resolved and are described comprehensively within the Ewald sphere concept. We show that the cone with apex angle α_2 is caused by the birefringence of the uniaxial crystal and, hence, can be expressed as a function of the ratio n_e/n_o of extraordinary and ordinary refractive indices. Remarkably, the scattering is found in poly- and mono-domain samples over a wide temperature regime up to 750 K, which excludes a relation of the scattering to ferroelectric domains or to photorefraction. The origin of the temperature-resistant refractive-index inhomogeneity yielding the scattering is related to a growth-induced seeding rod, i.e. a composition inhomogeneity primarily localized at the centre of the SBN sample. The rod is aligned parallel to the c axis and yields a refractive-index modulation with spatial frequencies on the micro-scale. Application aspects of the scattering, i.e. for phase-transition studies and for the determination of composition inhomogeneities, are discussed.

2. Experimental setup and results

Our investigations were performed in crystals of the polar oxide strontium barium niobate, $Sr_{0.61}Ba_{0.39}Nb_2O_6$ (SBN), which were grown by Rainer Pankrath using the Czochralski technique with resistance heating at about 1480 °C and slow pulling rates of about 0.8 mm h^{-1}. The samples were nominally pure or doped with Eu (4000 ppm Eu in the melt). The poly-domain samples were as grown. In order to obtain the mono-domain state, a field cooled poling procedure was applied [9]. The samples were cut along the principal axes of the tetragonal system with dimensions of approximately $a \times b \times c = (5 \times 5 \times 5)$ mm^3. All entrance faces of the samples were polished to optical quality. An Ar–Kr-ion laser providing wavelengths at $\lambda = 488$ and 647 nm served as an incident probe beam. According to figure 1 the unexpanded laser beam was adjusted under an external angle θ with respect to the crystal's c axis. The rotation stage allowed a precise angular adjustment of up to $\pm 0.1°$. Investigations were performed within an angular range of $0° < \theta < 90°$, choosing corresponding entrance faces. The beam power and light polarization were controlled by a half-wave retarder plate combined with a Glan–Thompson polarizer. The measurements were carried out with an intensity of 7 mW cm^{-2} at $\lambda = 488$ nm and 2 mW cm^{-2} at $\lambda = 647$ nm, respectively. The light polarization of the scattering was investigated with a polarization foil. Temperature-dependent measurements

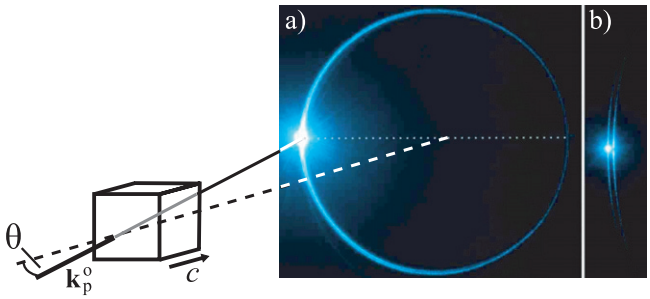

Figure 2. (a) Photograph of two bright sharp rings observed on a viewing screen for SBN:Eu with a probe beam at wavelength $\lambda = 488$ nm. Ordinary light polarization, $I = 7$ mW cm^{-2}. (b) Enlarged detail of the cones in the vicinity of the transmitted laser beam.

were performed up to about 750 K in a ceramic tube-shaped oven. The temperature at the surrounding of the crystal was measured by a thermocouple placed above the crystal through a small opening in the tube. The temperature could be measured with an accuracy of 5 K.

Figure 2 shows an example scattering pattern of the polydomain SBN:Eu crystal upon light exposure observed on a viewing screen at $\theta = (20.0 \pm 0.1)^\circ$ and at room temperature. The photographs were taken with a pump beam at $\lambda = 488$ nm and ordinary light polarization. Besides the directly transmitted laser beam, two bright sharp rings were observed. One ring of ordinary light polarization passed the directly transmitted laser beam and enclosed concentrically the second ring of extraordinary light polarization in the plane of incidence (see the enlarged detail in figure 2(b)). At the same time, both rings were found to be concentric with respect to the c axis. The rings originate from the intersection of two scattering cones with the viewing screen. The apex angles of the two cones were determined to be $\alpha_1 = (40.00 \pm 0.01)^\circ$ and $\alpha_2 = (39.85 \pm 0.01)^\circ$, respectively. The scattering appeared instantaneously with light irradiation.

Corresponding scattering cones appeared within an angular regime of $0^\circ < \theta < 90^\circ$. The apex angles $\alpha_{1,2}$ increased with increasing probe angle θ. Remarkably, a linear dependence $\alpha_1(\theta) = 2\theta$ was found. The angular dependence of α_2 is depicted in figure 3 via the difference $[\alpha_1 - \alpha_2](\theta)$. The measurement was performed with the probe beam entering the c surface of the sample. The accessible probe angle for transmission through both c faces was $\theta \approx \pm 60^\circ$.

For $\theta = 90^\circ$ the large apex angles of the cones yielded a sharp line of ordinary light polarization, as shown in figure 4(a). The rings did not appear for $\theta = 0^\circ$. In this particular case, a distribution of scattered light appeared around the directly transmitted probe beam, a scattering corona, as shown in figure 4(b).

Both the difference $[\alpha_1 - \alpha_2](\theta)$ and the intensity of the scattering cone with apex angle α_1 were investigated as a function of temperature in a range 290 K $< T <$ 750 K (see figure 5). For these measurements the wavelength $\lambda = 647$ nm was chosen to minimize the influence of the shifted absorption edge at higher temperatures [10]. For the blue wavelength ($\lambda = 488$ nm, see the lower inset in figure 5) the shift of the absorption edge results in a decrease in the scattering intensity in the high-temperature range.

Obviously, the scattering cones were observed in the red spectral range without noticeable intensity losses up to the maximum achievable temperature (see the upper inset in figure 5). The crossing point of the two cones, i.e. $[\alpha_1 - \alpha_2] = 0$, should be noted. At this temperature ($T_{bf} = (380 \pm 10)$ K for both wavelengths) the apex angle α_2 equals α_1 and the scattering intensity passes a minimum.

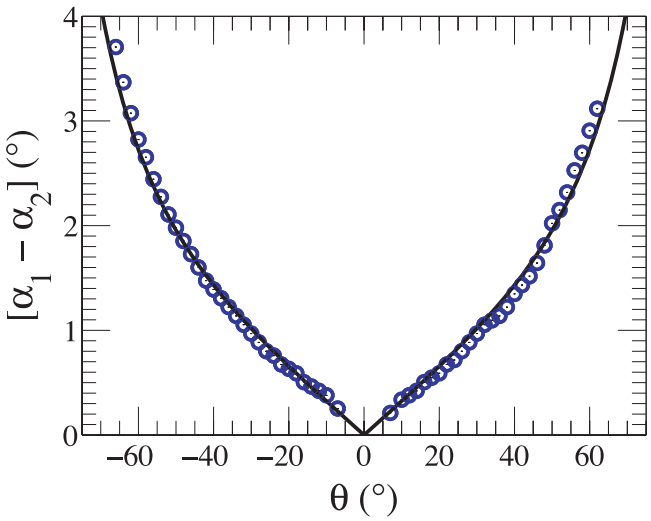

Figure 3. Experimentally determined difference $[\alpha_1 - \alpha_2]$ (circles) as a function of the probe angle θ. The solid line represents a fit of equation (4) to the experimental data.

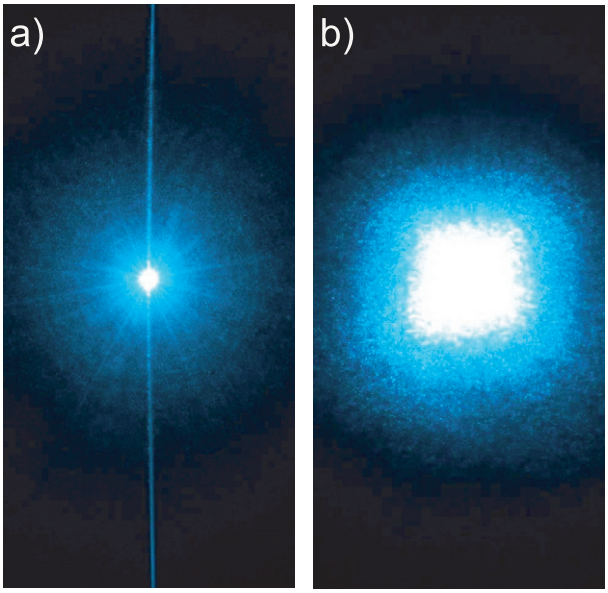

Figure 4. Scattering patterns for two special cases: (a) a line reflecting the large apex angles of the cones for $\theta = 90°$; (b) a symmetric corona for $\theta = 0°$.

Although the results presented here were gained with a polydomain Eu-doped SBN sample, all available mono- or polydomain, nominally pure or doped SBN crystals showed conical light scattering as well. We further note that the scattering cones also appeared with extraordinary light polarization of the probe beam. In this case, however, $(\alpha_1 - \alpha_2) < 0$ at room temperature.

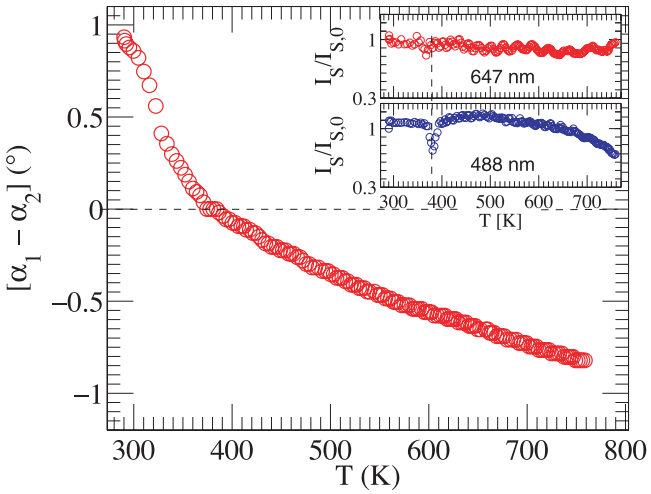

Figure 5. The apex angle difference $[\alpha_1 - \alpha_2]$ as a function of temperature for $\lambda = 647$ nm. θ was chosen to be 40°. The inset shows the normalized intensity of the scattering cone with α_2 for the two wavelengths $\lambda = 488$ and 647 nm.

3. Discussion

The two scattering cones discovered remind us of the photorefractive phenomenon of photoinduced polarization-anisotropic light scattering in cerium-doped SBN [4]. However, several key features for the appearance of the two cones cannot be explained in the frame of a photorefractive nonlinearity: (a) a poly-domain sample was used, so that a negligible macroscopic spontaneous polarization was present, i.e. negligible linear electro-optic tensor elements can be assumed; (b) the scattering cones were observed even in nominally pure samples of SBN, i.e. in crystals without the presence of a photorefractive centre with sufficient concentration; (c) the cones appeared instantaneously upon light exposure; (d) the cones could be observed up to temperatures of 750 K, i.e. far above the phase transition temperature in a regime where any residual spontaneous polarization vanished completely. In particular, in contrast to the photoinduced polarization-anisotropic scattering cone, ordinary light polarization of the probe beam was chosen. Additionally, the symmetry axes of the two cones coincided with the *c* axis and not with the transmitted probe beam.

From these features it becomes clear that the scattering pattern that we observed is fundamentally different from photo-induced light scattering. Likewise, we can exclude a relation of the scattering to the presence of needle-like ferroelectric 180° domains, as was discussed for non-collinear frequency doubling [6].

The experimental results inevitably point to the presence of an intrinsic inhomogeneity of the refractive-index on the micro-scale. The phenomenon therefore is more likely comparable with the scattering observed in natural tourmaline [1] where equivalent properties of the scattering cone are reported and the origin of the scattering is related to a cylinder-like microstructure in the crystal bulk formed by impurity ions.

Prior to discussing the origin of the scattering in SBN, we will examine the appearance of, in particular, two scattering cones, which has not been reported and analysed for conical light scattering up to now. For this purpose we regard the intrinsic refractive-index inhomogeneity on the micro-scale as a complicated diffraction grating. In the momentum space the grating can be linked to grating vectors $\mathbf{K}_j$ $(j = 1 \ldots n)$ distributed with random directions and lengths

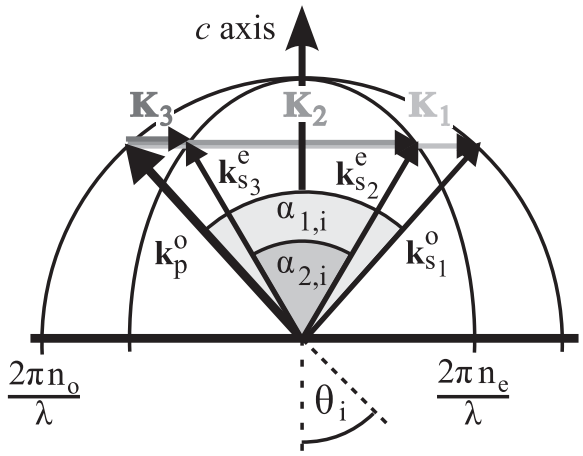

Figure 6. Ewald construction for the polarization-isotropic and -anisotropic scattering cones with apex angles $\alpha_{1,i}$ and $\alpha_{2,i}$. The subscript i denotes internal angles. The probe and scattered beams are denoted by the wavevectors $\mathbf{k}_p^{\mathrm{o}}$ and $\mathbf{k}_s^{\mathrm{o,e}}$, respectively. The presence of an intrinsic refractive-index inhomogeneity on the micro-scale is regarded as a complicated diffraction grating linked to grating vectors $\mathbf{K}_j$ $(j = 1 \cdots n)$ in momentum space.

within a plane normal to the c axis. As an example, three of the grating vectors are shown in the a–c-plane in the Ewald construction in figure 6.

Considering the plane of incidence, the ordinarily polarized probe beam with wavevector $\mathbf{k}_p^{\mathrm{o}}$ propagates under the internal angle θ_i with respect to the c axis. Ordinary and extraordinary refractive indices are indicated by n_{o} and n_{e}, respectively. One ordinarily polarized scattered wave $\mathbf{k}_{s_1}^{\mathrm{o}}$ and two extraordinarily polarized scattered waves $\mathbf{k}_{s_{2,3}}^{\mathrm{e}}$, respectively, appear according to the phase matching conditions:

$$\mathbf{k}_{s_1}^{\mathrm{o}} = \mathbf{k}_p^{\mathrm{o}} + \mathbf{K}_1 \tag{1}$$

$$\mathbf{k}_{s_2}^{\mathrm{e}} = \mathbf{k}_p^{\mathrm{o}} + \mathbf{K}_2 \tag{2}$$

$$\mathbf{k}_{s_3}^{\mathrm{e}} = \mathbf{k}_p^{\mathrm{o}} + \mathbf{K}_3 \tag{3}$$

with angles $\alpha_{1,i} = 2\theta_i$ and:

$$\alpha_{2,i} = 2\arctan(\pm n_{\mathrm{e}}/n_{\mathrm{o}} \tan\theta_i). \tag{4}$$

Equivalent considerations for the Ewald sphere concept in three dimensions consequently yield the appearance of two scattering cones with the same axis of rotation, the c axis. Obviously, ordinary light polarization results for the entire cone with apex angle $\alpha_{1,i}$, whereas extraordinary light polarization appears for the cone $\alpha_{2,i}$ in the plane of incidence only. The particular polarization state for any other scattering direction of $\alpha_{2,i}$ depends on the respective direction of the scattered waves.

For comparison with figure 3, the difference in the external angles $[\alpha_1 - \alpha_2](\theta)$ is expressed via the relations for the internal angles, $\alpha_{1,i} = 2\theta_i$, and equation (4), taking into account Snell's Law and the refractive indices from [11]. A fit of $[\alpha_1 - \alpha_2](\theta)$ to the experimental data is illustrated by the solid line in figure 3. The good agreement underlines the validity of the model that is presented. The ordinary refractive-index $n_{\mathrm{o}} = 2.3888$ at $\lambda = 488$ nm was taken from [11] for nominally pure, unpoled SBN, while n_{e} remained as a free fitting parameter. Here, it is assumed that the ordinary refractive-index of the Eu-doped SBN sample can be approximated by the values for the nominally pure samples. In contrast, the extraordinary

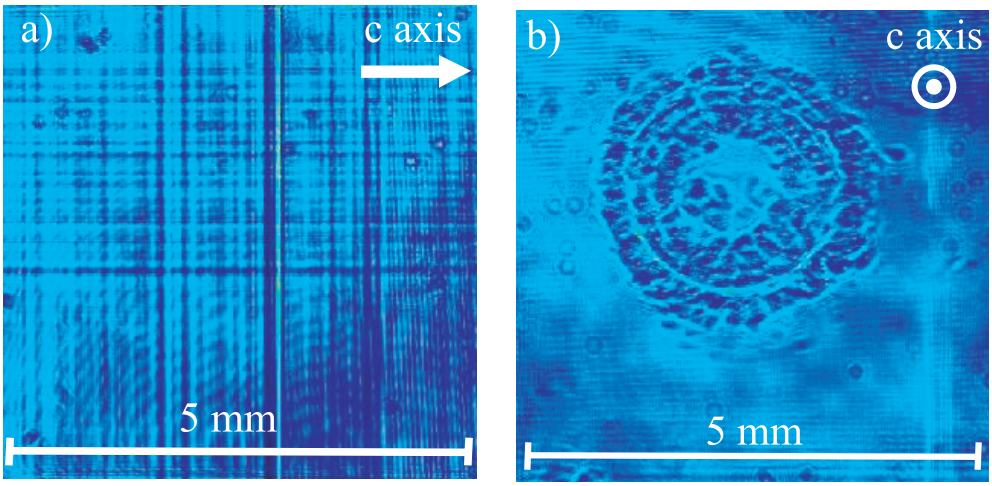

Figure 7. Topography of the transmitted intensity of an expanded extraordinarily polarized probe beam transmitting the SBN:Eu sample: (a) [100] and (b) [001] directions. Modulations of the detected intensity can be mapped onto local changes of the refractive-index.

refractive-index is expected to increase slightly due to the Eu doping. This assumption is reflected in the retrieved value of $n_e = 2.3695$ compared to $n_e = 2.3519$ ($\lambda = 488$ nm) for nominally pure samples [11].

The scattering patterns observed for the read-out angles $\theta_i = 0°$ and $\theta_i = 90°$, respectively (see figure 4), provide further insight into the properties of the wavevectors $\mathbf{K}_j$. For $\theta_i = 0°$, a scattering corona appears. This two-dimensional scattering pattern points to the presence of wavevectors $\mathbf{K}_j$ distributed with random directions and spatial frequencies within a plane normal to the c axis. This is stressed by the appearance of the scattering line in the case of probe beam propagation within the plane spanned by $\mathbf{K}_j$ ($\theta_i = 90°$). In this case, diffraction of the probe beam is restricted to directions normal to the c axis, yielding the sharp line of scattered light projected on the viewing screen.

We now address the origin of the scattering process. Obviously, the presence of wavevectors within a plane strictly perpendicular to the c axis in SBN reminds us of the **K**-plane reported in [6], explaining the appearance of non-collinear optical frequency doubling. The authors related the plane to the presence of ferroelectric 180° domains extended in the c direction along with a random distribution of the respective domain widths within the a–b-plane. They further assume that light scattering originates at domain walls, as discussed in [12–14], such that the scattering inevitably vanishes when passing the phase transition temperature. As we have already excluded a relation of the two scattering cones with the presence of ferroelectric domains, we can only suggest that scattering from domain walls and conical light scattering may coexist below T_M. The latter, however, exclusively remains in the regime $T \gg T_M$. This persistence of the refractive-index inhomogeneity to a temperature rise up to 750 K (and most probably to higher temperatures still below the melting temperature) underlines its intrinsic character in the crystal bulk. We hence inspected the homogeneity of the refractive-index of the crystal using intensity topography of an expanded extraordinarily polarized probe beam transmitting the sample. Figure 7 shows pictures of the transmitted light in the [100] and [001] directions for the SBN:Eu probe, taken with a charge coupled device (CCD) at a distance of 1 cm behind the sample. Modulations of the detected intensity originate from deteriorations of the transmitting light field due to light scattering and, hence, can be

mapped onto local changes of the refractive-index. We found two types of inhomogeneities, normal to and along the c direction. In the first case (see figure 7(a)), the inhomogeneity is due to growth striations, i.e. planes of equal composition which appear normal to c (parallel to the solid–liquid interface during growth) and can be influenced by the pulling and rotation rate [15]. In the second case, the inhomogeneity is marked by stripes parallel to the c axis (see figure 7(a)), which corresponds to the ring-shaped area in figure 7(b). This inhomogeneity can be assigned to the growth-induced seeding rod reported in [16].

Both inhomogeneities can be regarded as index gratings with particular sets of wavevectors $\mathbf{K}_j$ in the reciprocal space: the growth striations can be interpreted by wavevectors aligned parallel to the c axis and can be excluded as the source of the conical light scattering phenomenon according to the construction in figure 6. The growth-induced seeding rod, though, results in wavevectors of various lengths and orientations in a plane normal to the c axis. This inhomogeneity of the refractive-index can thus presumably be regarded as the origin of light scattering, yielding the two scattering cones. We note, however, that a definite assignment of the intensity topography to the scattering properties fails due to the limited spatial resolution (larger than λ) of the CCD.

The relation of the scattering to the growth-induced seeding rod strongly points to the relation of the scattering cones to a composition inhomogeneity of the SBN crystal on the micro-scale. In [17] the origin of the core was analysed by physical–chemical methods. It was found that the rod originates from hydrodynamic conditions in the melt during crystal growth, together with the defect structure of the seed crystal. As a result, changes in the Sr and Ba concentrations were detected in the rod area. Hence we can assume that the two scattering cones reflect spatial fluctuations of the Sr/Ba ratio on the micro-scale and that they therefore might be applied to visualize the presence of composition inhomogeneities. Another aspect in view of material analysis is reflected by the relation of the scattering cone α_2 to the ratio n_e/n_o. Our results show that n_e/n_o can be determined simply from the cone apex angle up to temperatures of 750 K. This aspect, in particular, enables phase-transition studies of SBN, i.e. investigations of the relaxor-ferroelectric behaviour in accordance with the powerful temperature-dependent studies of the birefringence [18, 19]. A first inspection of our experimental results yields $T_M = (331 \pm 10)$ K for the phase transition temperature and $T_D = (573 \pm 15)$ K for the Burns temperature, besides the temperature of zero birefringence $T_{bf} = (380 \pm 10)$ K. We would like to stress that the method allows investigation even in the case of poly-domain samples.

We finally add that we observed equivalent scattering cones in SBN crystals grown by the Stepanov technique [20] and in a wafer of Mg-doped $LiNbO_3$ as well. The intensities of the cones were weak in comparison with the intensities for the Eu-doped SBN sample but, again, they were strongly dependent on the probed volume fraction of the sample. This particularly was found with the Mg-doped $LiNbO_3$ wafer, where rather different areas could be probed, stressing the impact of the scattering cones for the purpose of wafer inspection. However, a systematic study of the scattering in $LiNbO_3$ is required in order to relate the scattering intensity to a composition inhomogeneity.

3.1. Conclusion

Concluding our results, conical light scattering is uncovered in poly- and monodomain, nominally pure and doped SBN crystals over a wide temperature regime. The appearance of two scattering cones, the scattering line and the corona is explained comprehensively within the Ewald sphere concept. The scattering can be attributed neither to photorefraction nor to scattering from domain walls nor from growth striations. The temperature-persistent scattering is assigned to an intrinsic inhomogeneity of the refractive-index on the micro-scale resulting

from a growth-induced seeding rod, i.e. a composition inhomogeneity primarily localized at the centre of the SBN sample. Therefore, the scattering can be applied for phase-transition studies of the relaxor-ferroelectric SBN up to temperatures as high as 750 K. The significant impact of our findings, however, is reflected by topographic investigations of the composition inhomogeneity via the scattering intensity. Furthermore, the scattering was found in Mg-doped $LiNbO_3$ as well, which makes the phenomenon applicable to a wide class of materials.

Acknowledgments

Financial support from the Deutsche Forschungsgemeinschaft (DFG) within the graduate school GRK 695, *Nonlinearities of optical materials*, and project IM 37/2-2 is gratefully acknowledged.

References

[1] Ja Y H 1990 A scattered ring in a natural crystal of tourmaline *J. Opt.* **21** 41
[2] van Olfen U, Rupp R A, Krätzig E and Grabmaier B C 1989 *Ferroelectr. Lett.* **10** 133
[3] Kasemir K-U and Betzler K 1999 *Appl. Phys.* B **68** 763
[4] Rupp R A, Seglins J and van Olfen U 1991 *Phys. Status Solidi* b **168** 445
[5] Imlau M, Woike Th, Schieder R and Rupp R A 1999 *Appl. Phys. Lett.* **75** 16
[6] Tunyagi A R, Ulex M and Betzler K 2003 *Phys. Rev. Lett.* **90** 243901
[7] Lemeshko V V and Obukhovsky V V 1995 *Ferroelectrics* **174** 249
[8] Forshaw M R B 1973 *Opt. Commun.* **8** 201
[9] Granzow T, Dörfler U, Woike Th, Wöhlecke M, Pankrath R, Imlau M and Kleemann W 2001 *Phys. Rev.* B **63** 174101
[10] Meyer M, Wöhlecke M and Schirmer O F 2000 *Phys. Status Solidi* b **221** R1
[11] Woike Th, Granzow T, Dörfler U, Poetsch C, Wöhlecke M and Pankrath R 2001 *Phys. Status Solidi* a **186** R13
[12] Kawai S, Ogawa T, Lee H S, DeMattei R C and Feigelson R S 1998 *Appl. Phys. Lett.* **73** 768
[13] Kleemann W, Licinio P, Woike Th and Pankrath R 2001 *Phys. Rev. Lett.* **86** 6014
[14] Volk T, Isakov D, Ivanov N, Ivleva L, Betzler K, Tunyagi A and Wöhlecke M 2005 *J. Appl. Phys.* **97** 074102
[15] Boniort J-Y, Brehm C, Desplanches G, Barraud J-Y and Margotin P 1975 *J. Cryst. Growth* **30** 357
[16] Ito Y, Kozuka H, Kashiwada Y and Furuhata Y 1975 *Japan. J. Appl. Phys.* **14** 1443
[17] Abramov N A, Ivleva L I, Kuz'minov Yu S, Myzina V A and Polozkov N M 1977 *Krist. Tech.* **12** 1157
[18] Bhalla A S, Guo R, Cross L E, Burns G, Dacol F H and Neurgaonkar R R 1987 *Phys. Rev.* B **36** 2030
[19] Lehnen P, Kleemann W, Woike Th and Pankrath R 2000 *Eur. Phys. J.* B **14** 633
[20] Ivleva L I, Bogodaev N V, Polozkov N M and Osiko V V 1995 *Opt. Mater.* **4** 168